Optics Letters

Fabrication of multipoint side-firing optical fiber by laser micro-ablation

Hoang Nguyen,[1] Md Masud Parvez Arnob,[2] Aaron T. Becker,[2] John C. Wolfe,[2] Matthew K. Hogan,[3] Philip J. Horner,[3] and Wei-Chuan Shih[1,2,4,5,*]

[1]Program of Materials Science & Engineering, University of Houston, Houston, Texas 77204, USA
[2]Department of Electrical & Computer Engineering, University of Houston, Houston, Texas 77204, USA
[3]Houston Methodist Research Institute, Houston, Texas 77030, USA
[4]Department of Biomedical Engineering, University of Houston, Houston, Texas 77204, USA
[5]Department of Chemistry, University of Houston, Houston, Texas 77204, USA
*Corresponding author: wshih@uh.edu

A multipoint, side-firing design enables an optical fiber to output light at multiple desired locations along the fiber body. This provides advantages over traditional end-to-end fibers, especially in applications requiring fiber bundles such as brain stimulation or remote sensing. This Letter demonstrates that continuous wave (CW) laser micro-ablation can controllably create conical-shaped cavities, or side windows, for outputting light. The dimensions of these cavities determine the amount of firing light and their firing angle. Experimental data show that a single side window on a 730 µm fiber can deliver more than 8% of the input light. This can be increased to more than 19% on a 65 µm fiber with side windows created using femtosecond laser ablation and chemical etching. Fine control of light distribution along an optical fiber is critical for various biomedical applications such as light-activated drug-release and optogenetics studies.   © 2017 Optical Society of America

Optical fibers are currently the primary medium to transmit light over long distances with negligible loss. Advantages over other signal-transferring cables include being impervious to electromagnetic interference, having faster speed, and less signal attenuation. Optical fibers also have a profound impact on many biomedical applications, including endoscopy, phototherapy, and optogenetics. However, traditional optical fiber design uses a linear, end-to-end approach in which light is coupled at one end and transmitted to the other end. Multiple light entry/exit points currently require a large cable bundle, which may cause permanent damage to the tissue during insertion. Therefore, a multipoint, side-firing optical fiber configuration would be more practical. Such a configuration could provide light distribution to a relatively large and targeted region to treat cancer in soft-laser therapy [1]. For example, the fiber can be placed under the skin to irradiate along a subsurface blood vessel. The side-firing configuration could also transmit light to hard-to-reach areas such as diseased tissues along sidewalls of tubular structures in the human body [2]. In optogenetics studies, the use of normal optical fibers is limited, since they can only transmit light to a single target [3–5]. That drawback can be overcome by using multipoint side-firing fibers, which provide 3D control of light delivery to stimulate selected neurons.

Inspired by a medical need for precise light-delivery in small areas, several techniques have been developed to build side-firing fibers [6,7]. Light exit points can be controlled using metal reflectors coated on the fiber's distal end to deflect the emanating light [2]. In another method, the fiber tip is beveled to refract light in different directions [2,8]. Arc discharge can be introduced for smoothening the beveled tip to reduce scattering and diffusion of the output light [9]. This technique is low cost, but it is difficult to achieve high precision. Other side-firing methods include surface-emitting fiber lasers [10], side-glowing fibers [11], and tilted fiber Bragg gratings [12]. Overall, most of these fabrication methods are still relatively complex, time-consuming, and expensive. Devices such as side-emitting fibers and side-glowing fibers have low output efficiency and poor localization of the illumination area.

Recent efforts have focused on forming cavities on the fiber bodies to alter light propagation inside the fiber core. For example, laser ablation was employed to pattern microstructures such as microholes and microchannels on the sides of both plastic and glass optical fibers for sensor applications [13–15]. Mechanical drilling [16] or laser-assisted chemical etching [17] can also provide similar microscale side holes on plastic optical fibers. These approaches illustrate the potential for three-dimensional light distribution alongside the fiber body, but this capability has not been fully investigated. This Letter shows laser ablation can be finely tuned to fabricate specific window geometries on the fiber body. This enables customized configurations of multipoint, side-firing, three-dimensional light distribution.

The fabrication process begins by fixing and positioning a 10 cm multimode glass optical fiber (BFL48-400, Thorlabs) on an acrylic substrate. A commercial CO_2 laser (Universal Laser Systems VLS 3.50) with a wavelength of 10.6 μm and maximum CW power of 50 W was used for ablation, a precise removal of glass material that permanently changes the structure of the fiber core. During the fabrication process, the fiber samples remained stationary while the laser beam scanned along the fiber axis under computer control (Universal Control Panel software). At sufficiently high laser power, phase transformation occurred inside the fiber core. In silica-based materials ablation occurs at the heat-affected zone when the irradiance exceeds ~10^5 W/cm² [18]. Increasing irradiation time resulted in deeper penetration into the fiber. By ablating with 50 W, 20% speed, 1000 dpi resolution, a ~260 μm wide and ~135 μm deep crater-shaped side window was created with the two outer layers completely removed and the core partly removed, as shown in scanning electron microscopy (SEM) images in Fig. 1.

Side-firing of light from the ablated window is achieved through total internal reflection (TIR), as shown in Fig. 2 (a). The light inside the fiber is reflected at the angled surface of the side window because the incident angle exceeds the TIR angle. A simulation model has been employed elsewhere [19] to demonstrate the effect of the side-window's geometry on the side-firing light. Side-firing also occurs in an aqueous medium, indicating that these fibers can be employed for *in vivo* applications such as laser treatment of the urethra. In this
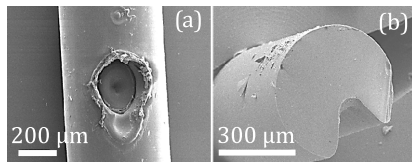

Fig. 1. SEM image of the light window fabricated by a 50 W CW laser. (a) Top view of the side window with buffer and cladding layers intact. (b) Cross section of the side window without the buffer and cladding layers.
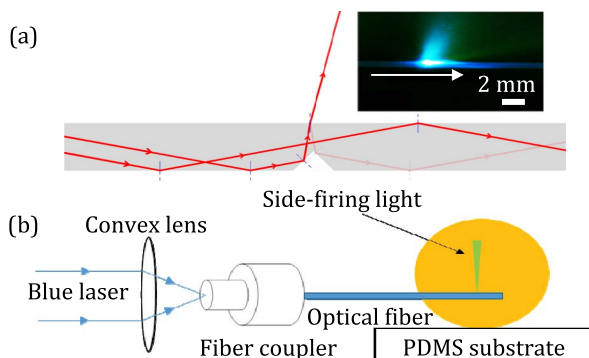

Fig. 2. (a) The crater-shaped window causes the input light incident angle to exceed the TIR critical angle, thus part of the input light refracts through the fiber; top right: side-firing light profile in acridine orange solution. The white arrow indicates the direction of blue laser light (473 nm) inside the fiber. (b) Optical setup used to take the fluorescent profile image of the side-firing light from the window.
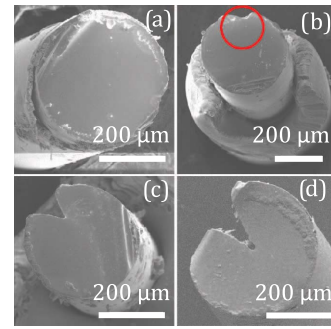

Fig. 3. Cross section of the fiber core after ablation with different laser powers. The window increased in both width and depth when ablated with increasing laser power. (a) Laser power at 10 W, no visible change on the fiber core; (b) at 20 W, a small dent appears on the core (red circle); (c) at 30 W, the laser started ablating a large portion of the core; (d) deeper window at 40 W.

experiment, a fiber section with one side window was immersed in acridine orange solution; the other end was inserted into a multimode fiber connector (B10440A, Thorlabs). The connector was then attached and locked into a bare fiber terminator (BFT1, Thorlabs) mounted on a metallic stage. A 473 nm laser output (Mai Tai HP, Spectra-Physics) was focused by a convex lens (*f*:50 mm) into the fiber core. This setup achieved an optical coupling efficiency of ~80% with negligible transmission loss.

The geometry of the side window can be precisely controlled by adjusting the laser power. As shown in Figs. 3 and 4(a), the width (●) and depth (■) of the window correlate with the laser power. Interestingly, the light exit angle also correlates with the window geometry, indicating the ability to fully manipulate
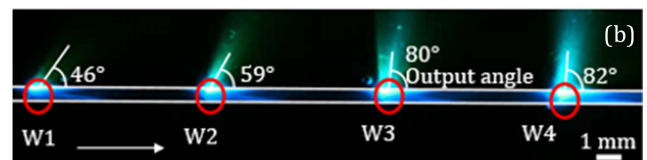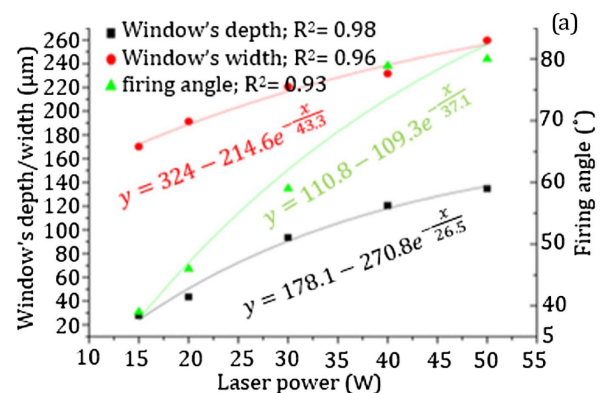

Fig. 4. (a) Side window's dimension and firing angle fabricated at different laser powers. (b) Fluorescent profile of side-firing light from an optical fiber with four windows in acridine orange solution. Red circles show the position of each side window. The white arrow indicates the light direction in the fiber. The distance between each window is 8 mm.
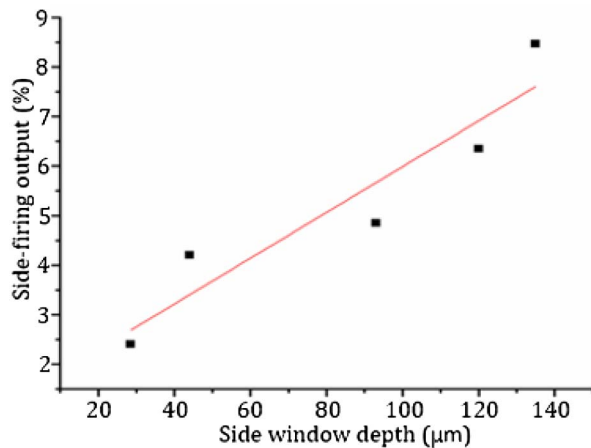
Fig. 5. Side-firing output from windows at different depths. The side window depth was controlled by tuning the power of the ablating CW laser.

the propagating light direction via the laser ablation process. As shown in Fig. 4(b), the fluorescence emission of the acridine orange solution reveals different launch angles (▲) for four windows: W1, W2, W3, and W4 ablated with 20, 30, 40, and 50 W, respectively. The launch angle is ~46° for W1, ~59° for W2, ~80° for W3, and ~82° for W4. Approximately 8% of the total coupled light inside the fiber core exited through a single window ablated by 50 W CW laser power measured by a handheld laser power meter (Ophir 7Z01500). Figure 5 illustrates that the output light power is proportional to the laser ablation power. This occurs because higher ablation power creates larger windows that allow more light to exit. In this set of experiments, up to 20% of the total coupled light exited from a single window after multiple ablations. It is noted that the deeper side window reduces the fiber's mechanical strength, so the depth and mechanical strength are an engineering trade-off whose solution is application specific. We note that the exponential fits in Fig. 4(a) and linear fit in Fig. 5 are meant to provide an empirical understanding of how the fabrication process behaves for later design purposes. Rotating the optical fiber sample on the substrate enables placing multiple windows in close axial distance but different radial directions along the fiber axis, resulting in a 3D, side-firing configuration (Fig. 6). This three-dimensional design provides the ability to generate 3D light delivery using a single fiber.

100 μm is the smallest feature that can be fabricated onto optical fibers with the CW CO_2 laser instruments designed for general cutting and engraving. These lasers generate a large
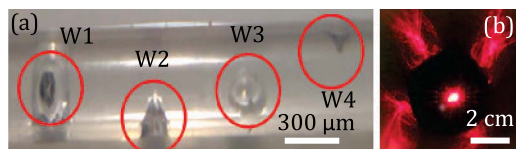

Fig. 6. (a) Four windows W1–W4 (red circles) positioned along the fiber axis at orientations of 0°, 90°, 180°, and 270° difference. (b) The 3D light configuration from these four windows. The fiber was coupled with a He–Ne laser ($\lambda = 633$ nm) and placed inside a conical frustum to image the side-firing light profile.

heat-affected zone, preventing use on optical fibers smaller than 300 μm in diameter. Smaller fibers are desirable for many applications. For example, reducing the diameter of an optical fiber inserted into biological tissue reduces potential tissue damage. Laser-ablated feature size can be scaled down by using shorter pulses.

Therefore, for optical fibers with diameters less than 100 μm, a Ti-sapphire mode-locked femtosecond (fs) laser with 100 fs laser pulses (820 nm) and a repetition rate of 80 MHz (Mai Tai HP, Spectra-Physics) was used in this set of experiments. 65 μm outer diameter (OD) optical fibers (Polymicro Technologies, FVP050055065) with a 50 μm silica core containing a high concentration of hydroxyl (OH) groups, 2.5 μm doped silica cladding, and a 5 μm polyimide buffer jacket were used for fabricating side-firing windows. At a high repetition rate of 80 MHz, the fs pulse duration and time interval between each successive laser pulse are far shorter than the time scale for heat diffusion out of focal volume (1 μs) [11]. Thus, the accumulation of energy deposited by each laser pulse generates localized ablation in the focal region. Focusing the laser beam through an objective lens to a sufficiently small spot on the fiber body allows the formation of submicron features.

High-energy laser pulses would destroy the surrounding buffer layer completely, resulting in a very brittle section. In contrast, low-energy laser pulses and chemical etching were employed to minimize the damage caused on the buffer layer. The laser pulse energy was adjusted to ~0.5 nJ to ablate 5 μm diameter, circular-shaped windows on the buffer layer, thereby exposing the silica cladding [Fig. 7(a)]. Then, the fiber sample was immersed in a buffer hydrofluoric (HF) acid bath to etch the cladding and the core. The etch rates for the cladding layer and the core were determined to be ~83 nm/min and ~73 nm/min, respectively. This process resulted in crater-shaped windows, as shown in Fig. 7(b). Testing data show that one window on the 65 μm optical fiber can emit up to ~25% of the total coupled light. This is a higher efficiency than with 730 μm fibers because small fibers have a higher optical power density. However, as HF etching resulted in a rough interface for the side window, it also increased the scattering of the reflected light. Because of this, the side-firing light profile of a 65 μm fiber has a wider spread angle, as shown in Fig. 7(c). A narrower range of light delivery angle can be achieved by
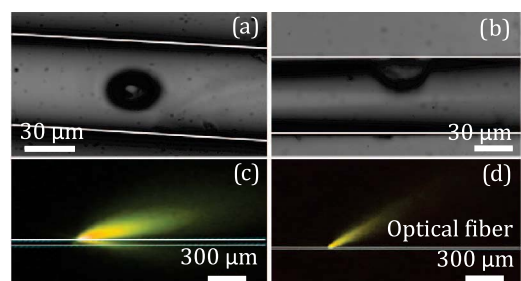

Fig. 7. (a) 5 μm opening hole on the buffer layer of a 65 μm fiber to expose the silica cladding. (b) Crater-shaped window created by buffer HF etching through the hole. (c) Wide side-firing light profile after buffer HF etching. (d) Narrow side-firing light profile after gold coating. Fiber samples were coupled with green laser light (532 nm) and immersed in the R6G solution. White lines are used to outline the fiber. White arrows indicate the light propagation direction in the fiber.
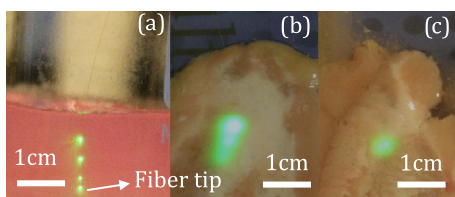
Fig. 8. (a) 65 μm OD side-firing optical fiber with three windows tested in the agar model of brain tissue. (b) Side view of the same fiber inserted in a swine brain slice shows a larger illuminated volume inside the tissue. (c) Side view of unmodified 65 μm fiber in a swine brain slice shows smaller illuminated volume localized at the tip of the fiber. Illumination sites in the swine brain were observed through an ~0.5 cm layer of brain tissue.

sputter coating a thin layer of gold on the opening side of the window [Fig. 7(d)]. However, the coating reduces the power of the output, resulting in a trade-off between power output and localized delivery.

The 65 μm multipoint side-firing optical fiber can be employed for *in vivo* optogenetic brain neuron stimulation. This requires the ablated fibers to perform well in tissue media. Experiments conducted in an agar-based brain tissue model (0.5% m/v in water) show the observed light exiting from the three side-firing windows [Fig. 8(a)]. Further experiments on swine brain tissues showed that a side-firing fiber could illuminate a larger volume [Fig. 8(b)] compared with unmodified fiber [Fig. 8(c)] when inserted into the tissue. These experiments demonstrated the effectiveness of side-firing fiber in biological tissue. The fiber's mechanical strength was also tested via the agar experiments. Fibers with side window depth of more than half of the fiber core diameter has its strength significantly reduced and are more prone to break during insertion. A method to restore the fiber strength by dip coating the fiber in a transparent polymer is under development.

In conclusion, this Letter presents a 3D, multipoint, side-firing optical fiber to control the launch direction and distribution of light in brain tissue. It can be used effectively as a light delivery device for optogenetics stimulation and for soft-laser therapy. The multisite localization ability of the fiber can also be used to activate light-sensitive chemical reactions and thermal responses. This side-firing fiber reduces the need for multiple linear end-to-end fibers, potentially reducing the time required for a procedure, avoids the need to reposition the fiber to different regions, and causes minimal tissue damage.

Other potential applications such as distributed remote sensing technology can also be envisioned by operating in the reverse lightpath, i.e., collecting signals from multisites to a single detector.

REFERENCES

1. J. Spigulis, J. Lazdins, D. Pfafrods, and M. Stafeckis, Med. Biol. Eng. Comput. **34**, 285 (1996).
2. C. F. B. van Swol, R. M. Verdaasdonk, R. J. van Vliet, D. G. Molenaar, and T. A. Boon, World J. Urol. **13**, 88 (1995).
3. S. T. Lin, J. C. Wolfe, J. A. Dani, and W. C. Shih, Opt. Lett. **37**, 1781 (2012).
4. S. T. Lin, M. Gheewala, J. C. Wolfe, J. A. Dani, and W. C. Shih, Proc. IEEE **5**, 700 (2011).
5. N. Zorzos, E. S. Boyden, and C. G. Fonstad, Opt. Lett. **35**, 4133 (2010).
6. U. Utzinger and R. R. Richards-Kortum, J. Biomed. Opt. **8**, 121 (2003).
7. C. Kim, H. Park, and H. Lee, Lasers Surg. Med. **45**, 437 (2013).
8. S. H. Lee, Y. T. Ryu, D. H. Son, S. Jeong, Y. Kim, S. Ju, B. H. Kim, and W. T. Han, Opt. Express **23**, 21254 (2015).
9. I. B. Sohn, Y. Kim, Y. C. Noh, I. W. Lee, J. K. Kim, and H. Lee, Opt. Express **18**, 19755 (2010).
10. O. Shapira, K. Kurichi, N. D. Orf, A. F. Abouraddy, G. Benoit, J. F. Viens, A. Rodriguez, M. Ibanescu, J. D. Joannopoulos, Y. Fink, and M. M. Brewster, Opt. Express **14**, 3929 (2006).
11. J. Spigulis, D. Pfafrods, M. Stafeckis, and W. Jelinska-Platace, Proc. SPIE **2967**, 231 (1997).
12. G. Wang, C. Wang, Z. Yan, and L. Yang, Opt. Lett. **41**, 2401 (2016).
13. L. Athanasekos, M. Vasileiadis, A. E. Sachat, N. A. Vainos, and C. Riziotis, J. Opt. **17**, 015402 (2015).
14. I. Sohn, Y. Kim, and Y. Noh, J. Opt. Soc. Korea **13**, 33 (2009).
15. R. Irawan, T. S. Chuan, T. C. Meng, and T. K. Ming, Bentham Open **2**, 28 (2008).
16. G. Liu, D. Feng, M. Zhang, S. Jiang, and Z. Ye, IEEE Sens. J. **15**, 2902 (2015).
17. R. Yand, Y. S. Yu, C. Chen, Q. D. Chen, and H. B. Sun, Opt. Lett. **36**, 3879 (2011).
18. C. B. Schaffer, J. F. Garcia, and E. Mazur, Appl. Phys. A **76**, 351 (2003).
19. A. T. Becker and H. Nguyen, "Defects in an optical fiber," http://demonstrations.wolfram.com/DefectsInAnOpticalFiber/, Wolfram Demonstrations Project, October 2016.